Acta Technica Napocensis: Civil Engineering & Architecture Vol. 60, No. 2 (2017)
Journal homepage: http://constructii.utcluj.ro/ActaCivilEng

Durability of Recycled Aggregate Self-Curing Concrete

Bashandy A. A. *(1), Safan M. A.(1), Ellyien M. M. (2)
(1) Associate Professor at Civil Engineering Department, Faculty of Engineering, Menoufia University, Egypt.
(2) Professor at Civil Engineering Department, Faculty of Engineering, Menoufia
(2) Civil Engineer, M.Sc. Candidate

(Received 26 September 2017, Accepted 3 December 2017)

ABSTRACT

Recycled aggregate self-curing concrete is a one of innovative concretes that can be cured without using conventional curing regimes. It is made from coarse recycled aggregates instead of natural coarse aggregates. Recycled aggregates can store a high amount of water that is not part of the mixing water to create water supply reservoirs in the concrete to continue the hydration process. In this investigation, the durability of recycled aggregate self-curing concrete studied under the attack of sulfates and chlorides. The effect of sulfates on compressive, splitting tensile and flexure strengths at different ages (2, 4 and 6 months) is studied. The effect of chloride attack (as 8% concentrated sodium chloride solution) is studied on bond and flexure strengths at different ages (1 and 2 months). Also, the flexure behavior of the recycled aggregate self-curing reinforced concrete beams is studied individually and under the effect of chloride attack after different exposure periods. Test results indicated that using recycled aggregates (such as crushed concrete and crushed red bricks) can be used in self-curing concrete with satisfied durability characteristics under chlorides and sulfate attacks. Dolomite then crushed concrete followed by crushed red bricks can be used as coarse aggregates for self-curing concrete.

Keywords: *Durability; Self-curing; Recycled aggregate; Polyethylene Glycol; Superplasticizer; Concrete.*

1. INTRODUCTION

Use of recycled materials as aggregates in civil engineering applications is beneficial because it reduces the environmental impacts and cost of obtaining concrete.

The most significant difference in the physical properties of coarse recycled concrete aggregates RCA reflected in most studies is its higher water absorption capacity as compared to coarse natural aggregates due to the higher porosity of the mortar adhered onto the aggregate in the RCA. The smaller the size of RCA, the higher values of adhered mortar, the high water demand of concrete mixture due to the high porosity of adhering mortar [1-4]. [1,2,3,4]**.**

Concrete curing is one of the most important processes in achieving the desired properties of the concrete. Self-curing concrete represents a new trend in the concrete curing methods. The basic concept of this technology is to provide water for concrete so that it can continue the curing process on its own. This is done by embedding the water inside the materials used to make concrete or/and reducing the water evaporation from the concrete and hence increase the water retention capacity of concrete. This technology can reduce but not to completely remove the drying shrinkage. Furthermore, compressive strength will be enhanced with the reduced shrinkage arising from water evaporation, making it ideal for concrete placing without any external curing [5-12]. [5,6,7,8,9,10,11,12]**.**

Shrinkage-reducing admixture (SRA), based on the use of poly-glycol products in the concrete mixes, has been more recently suggested to reduce the risk of cracking in concrete structure caused by drying shrinkage. The mechanism of this admixture is based on a physical change (reduction of the surface tension of the mixing water) rather than on a reduction of water evaporation [13].

Durability is defined as the capability of concrete to resist deterioration from an external environment [14]. Recycled aggregate is more porous compared to natural aggregate, increased porosity of recycled aggregate may lower the bond strength between the cement paste and the aggregate (interfacial transition zone), thereby leading to a loss in concrete strength, an increase in ion penetrability and presumably a reduction in corrosion resistance [15].

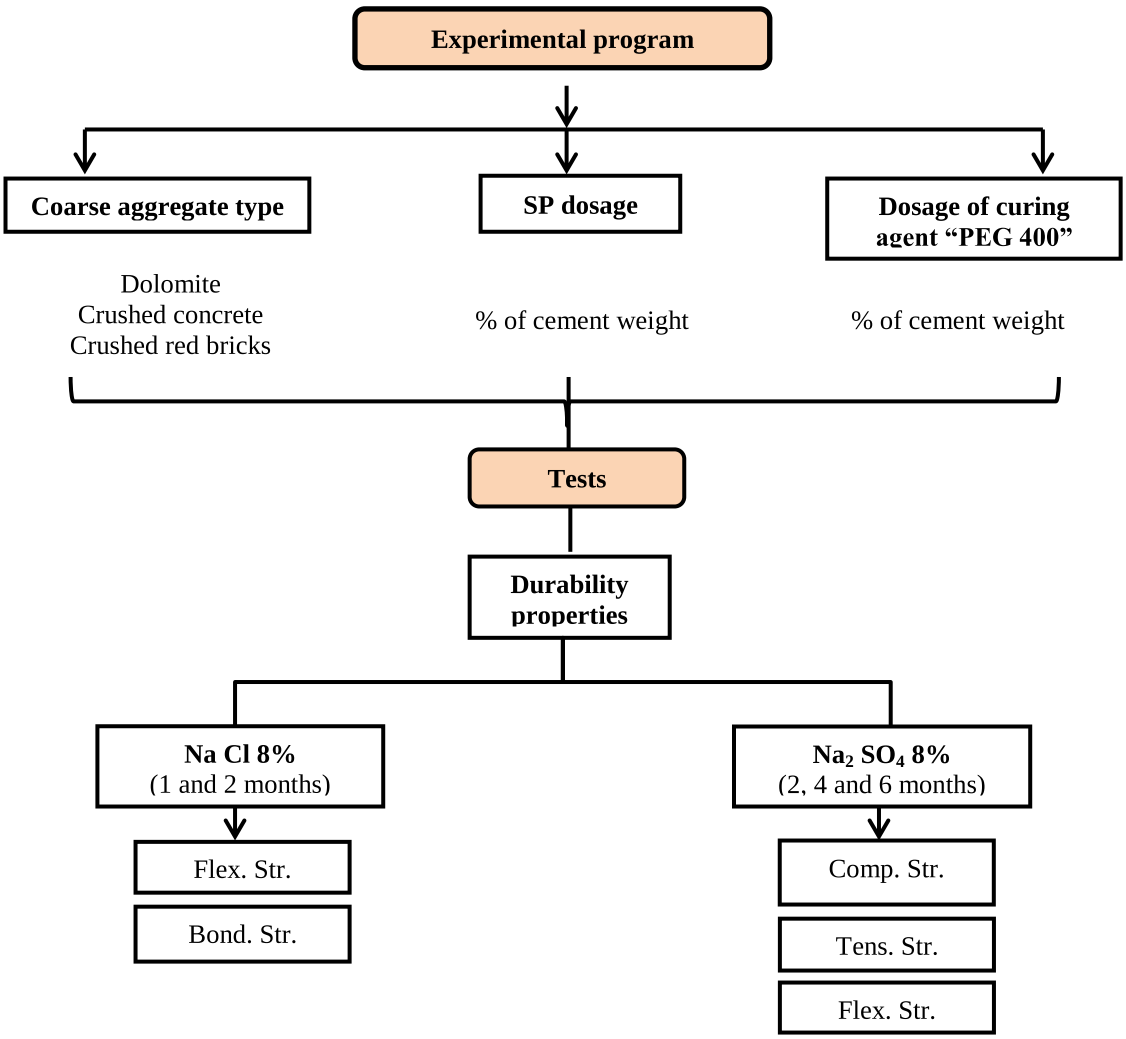

Fig. 1. Experimental Program.

Internal curing was investigated as a potential method to improve the durability of Recycled Aggregates Concrete (RAC). Crushed concrete aggregates (CCA) have potential as an internal curing agent due to its high absorption capacity and low cost. Utilization of crushed recycled concrete aggregates (CRCA) as internal curing agent resulted in a limited reduction in autogenous shrinkage of high-performance mixtures [16,17]. In this research, the durability of recycled aggregate self-curing (RA-SC) concrete is studied.

2. RESEARCH SIGNIFICANCE

The main aim of this research is to study the durability of recycled aggregate self-curing (RA-SC) concrete. The durability is studied under the attack of sulfates and chlorides (Na_2SO_4 and NaCl with a concentration of 8%). The sulfate effects were studied for main mechanical hardened properties of concrete samples after 2, 4 and 6 months. The chloride effects were studied for standard cubes with embedded rebars and reinforced concrete beam samples after 1 and 2 months. Beam samples immersed in sodium chloride solution (with 8% concentration degree) then connected to an electrical cell to accelerate the chloride effects. The flexure behavior of the RA-SC reinforced concrete beams is studied.

The importance of this research is based on current research needs to know the data addressing the long-term behavior of recycled aggregate self-curing concrete. This research provides data for the engineers concerning the influence of using self-curing concrete cast using recycled aggregate as a green concrete in aggressive conditions, which contains chloride and sulfate ions.

3. MATERIALS AND TEST SPECIMENS

All tests in this research are carried out in the Construction Materials Laboratory in Civil Engineering Department, Faculty of Engineering, Menoufia University.

The materials used, design of test specimens and testing procedures are discussed in the following sections. The conducted experimental program is shown in Fig. (1).

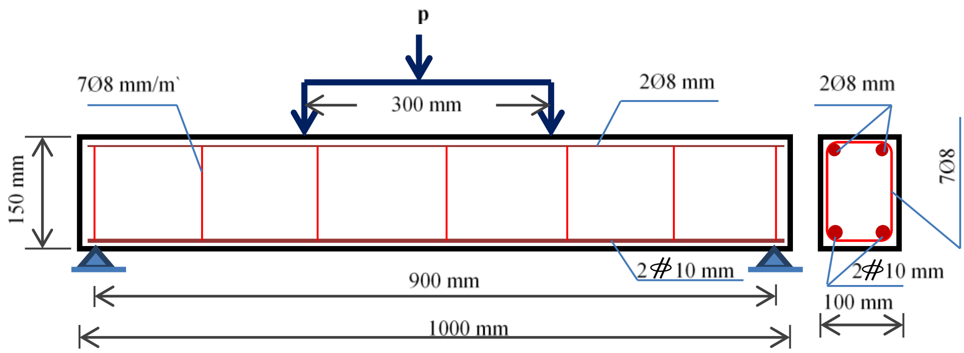

Fig. 2. Dimensions, reinforcement and the loading method for beam sample.

3.1. Materials

Cement: The cement used is the ordinary Portland cement CEM I 42.5 N from the Suez cement factory. It satisfies the Egyptian Standard Specification for cement [18].

Water: Drinkable clean water, fresh and free from impurities is used for mixing according to the Egyptian code of practice [19].

Fine aggregate: The fine aggregate used is the natural siliceous sand that satisfies the standards for concrete aggregates [20]. It is clean and nearly free from impurities with a specific gravity 2.6 and a fineness modulus of 2.61. Its mechanical properties are shown in Table (1) while its grading is shown in Table (2).

Table 1. Physical properties of the sand used.

Property		Value
Specific gravity		2.6
Volumetric weight	*(t/m^3)*	1.73
Voids ratio	*(%)*	33.81
% absorption	*(%)*	0.78

Table 2. Sieve analysis of the sand used according to (ASTM C33).

Sieve size (mm)	9.5 mm	4.75 mm	2.36 mm	1.18 mm	0.61 mm	0.31 mm	0.16 mm
% Passing sand used	100	100	94	80	50	15	0

Coarse aggregate: Two types of aggregates are used, natural and recycled aggregates. The coarse aggregate used are crushed dolomite with a maximum nominal size of 20 mm and recycled aggregate (crushed red brick and crushed concrete) as shown in Table (3) and (4). It satisfies the ASTM C-33 [20]. The shape of these particles is irregular and angular with a very low percentage of flat particles.

Table 3. Physical properties of the dolomite, crushed concrete and crushed red bricks used.

Property		Dolomite	Crushed concrete	Crushed red bricks
Specific gravity		2.64	2.5	1.6
% Absorption	(%)	0.76	4	10
Aggregate crushing value (ACV)	(%)	17.5	30	50

Table 4. Sieve analysis of the dolomite, crushed concrete and crushed red bricks used according to (ASTM C-33).

Sieve size (mm)	25 mm	19 mm	9.5 mm	4.75 mm	2.36
% Passing ASTM C-33	100	90-100	20-55	0-10	0-5
% Passing Dolomite	100	98	25	1	1
% Passing crushed red bricks	100	100	30	2	1
% Passing crushed concrete	100	100	40	2	1

Fig. 3. Electrical cell [25].

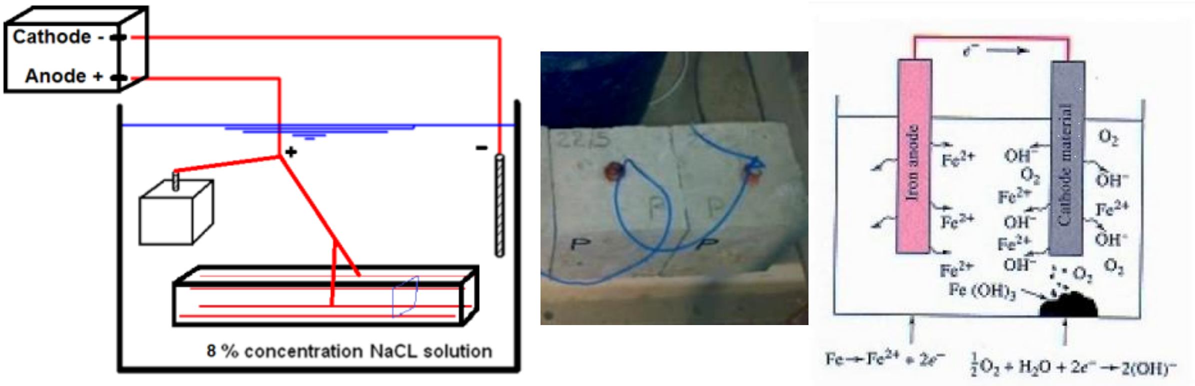

Fig. 4. Electrical circuit to accelerate the corrosion at cubes and beams.

Steel Rebars: Two types of steel rebars are used, mild and high tensile steel rebars. Mild steel bars of 8 mm diameter were used for stirrups with yield strength of 240 MPa and had a tensile strength of 350 MPa. Its chemical and physical characteristics satisfy the Egyptian Standard Specification E.S.S. 262/2011 [21]. High tensile deformed steel bars produced from the Ezz Al Dekhila Steel at Alexandria were used. Deformed high tensile steel bars of grade 360/520 with a nominal diameter of 12 mm and a length of 160 mm were used as embedded reinforcement with a proof stress of 360 MPa. Steel bars of diameter 10 mm were used in reinforcing the concrete beams as shown in Fig. (4). Their yield stress was 380 MPa and their tensile strength was 570 MPa. Its chemical and physical characteristics satisfy E.S.S. 262/2011 [21].

Admixtures:

Chemical admixture: A high range water reducing (HRWR) admixture is often referred to as superplasticizer (Sika ViscoCrete® -5930 L) to help in increasing the workability of concrete without an additional amount of water. It meets the requirements of ASTM-C- 494 Types G and F [22]. Its main properties are shown in Table (5). Superplasticizer (Sika ViscoCrete® -5930 L) is obtained from Sika Company.

Table 5. Technical information about SP (Viscocrete 5930 L) used *(As Provided by Manufacturer)*.

Base	Appearance	Density	Chloride content	Air entrainment	Compatibility
Aqueous solution of modified poly carboxylate	Turbid liquid	1.08±0.005 kg/liter	Nil	Nil	All types of Portland cement

Table 6. Technical information about Polyethylene Glycol 400 "PEG400" used *(as provided by manufacturer).*

PEG type	Average molecular weight	Hydroxyl Number, Mg KOH/g	Liquid Density, g/cc			Melting or Freezing range °C	Solubility in Water at 20°C, % by weight	Viscosity at 100°C,
			20 °C	60°C	80°C			
PEG 400	380 to 420	264 to 300	1.1255	1.0931	1.0769	4 to 8	Complete	7.3

Self-curing agent: In this study Polyethylene glycol PEG400 is used as a chemical agent in a liquid form for internal curing of concrete. It is free of chlorides and produces an internal membrane, which protects and prevents fresh concrete against over-rapid water evaporation. Table (6) showed the characteristics of Polyethylene-glycol PEG400 as produced by the manufacturer. It is produced by Morgan Chemicals Pvt. Ltd in Egypt.

3.2. Concrete and Test Samples

Concrete mixes were chosen based on the previous researches [23,24]. Table (7) shows the proportions of recycled aggregate self-curing RA-SC concrete mixes used to study the effect of sulfates and chlorides on the durability of RA-SC concrete.

The conducted experimental program is shown in Fig. (1). The durability behavior of self-curing concrete samples cast using natural aggregates compared to self-curing concrete samples cast using recycled aggregates is studied. The using of crushed concrete and crushed red bricks compared to using dolomite as coarse aggregates is evaluated. The ordinary Portland cement, graded sand, suggested coarse aggregate types, superplasticizer, and chemical curing agent "PEG400" as a percentage of cement weight.

Table 7. Proportions of concrete mixes used [24].

Mix code	Materials									Tested samples			Curing method
	C (kg)	W (kg)	F.A (kg)	C.A		S.P		P.E.G		Compressive strength	Tensile strength	Flexure strength	
				Type	Weight (kg)	%	Weight (g)	%	Weight (g)				
DS	350	175	615.92	Dolomite	1231.84	0.75%	2625	0.25%	875	12 Cubes 10*10*10 cm for each Mix.	12 cylinders 10 * 20 cm for each Mix.	12 prisms 10*10*50 cm for each Mix.	Self-Curing using P.E.G 400
CS	350	175	599.92	Crushed concrete	1199.85	0.75%	2625	0.25%	875				
BS	350	175	434.79	Crushed Brick	869.58	0.5%	1750	0.5%	1750				

The specimens used in this study are cubes of 100x100x100 mm to get the compressive strength; cylinders of 100x200 mm to determine the splitting tensile strength, prisms of dimensions of 100x100x500 mm to determine the flexure strength, cubes of dimensions of 150x150x150 mm with embedded rebars of ∅12 mm to determine the bond strength. Reinforced concrete beams having the dimensions of 100x150x1000 mm are cast to study the flexure behavior of beams as shown in Fig. (2). Each beam was reinforced with 2 ∅10 mm of high strength steel (St. 52) as main lower reinforcement and 2Ø8 mm of mild steel (St. 37) as stirrup hunger with stirrups of 7Ø8/m' as shown in Fig. (2). The concrete was placed in timber molds. In order to have good compaction of the concrete mix, the electric vibrator was used. Finally, their surfaces were finished with a trowel. To test them, the beam specimens were placed on a flexure testing machine of a capacity of 100 KN as shown in Fig. (4). Two deflectometer dial gauges were used (at mid and quarter points of lower surface) to determine the deflections of the reinforced "RA-SC" concrete beams. The demec points were used to measure the strain values. They were fixed on the side surface of the tested concrete beams as shown in Fig. (4). A strain gauge was used to determine the tensile and compressive strain values for the reinforced "RA-SC" concrete beams.

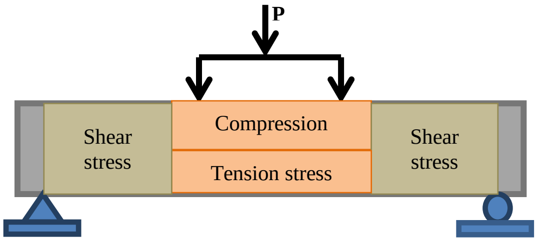

Fig. 5. Four point load flexure tests.

Flexure strength for prisms

Flexure strength for beams

Fig. 6. Flexure strength test for prisms and beams**.**

A schematic sketch showing the positions of strain measurement on the specimen is presented in Fig. (5). Beams were tested and the deflection values, as well as compressive and tensile strain values, were determined. Initial crack load and failure loads were recorded and crack patterns are sketched.

3.3. Sulfate Attack Simulation

To simulate the sulfate attack, the samples are immersed in 8% concentration Na_2SO_4 solution for periods up to 6 months. All samples are immersed then tested after 2, 4 and 6 months. Results are compared to control samples. The tested samples are standard cubes, cylinders, and prisms to obtain compressive, splitting tensile and flexure strength values. The effects of sulfate attack are obtained in terms of compressive, splitting tensile and flexure strengths.

3.4. Chloride Attack Simulation

In this test program, the simulation of chlorides attack was performed by immersing the samples in 8% concentration NaCl solution for 2 months. Tested samples are standard cubes with embedded rebars *(as discussed before)* and reinforced concrete beam samples as shown in Fig. (2). An electrical cell was used to accelerate the corrosion process for a period of two months [25] as shown in Fig. (3). Steel rebars are joined to the electrical cell as shown in Fig. (4). The embedded rebars are connected to the positive anode. Steel peace connected to the negative cathode then immersed in the same solution as shown in Fig. (4). Ions leave the surface of the steel reinforcing bars and pass into the water. Fresh atoms ionize to replace the desorbed ions. The steel rebar corrodes. The electrons released by the ionized iron atoms flow through the connecting wire to the cathode bar. At the cathode bar, the released electrons which have built up attracts positive hydrogen ions. The hydrogen ions are adsorbed onto the bar's surface and then combine with the electrons to form hydrogen gas. The gas bubbles up and leaves the solution. The cathode bar does not corrode. It simply provides a surface where hydrogen ions can meet and combine with electrons [25-26]. [26,27,25].

Electrons keep on flowing around the wire until all the rebars have corroded away or until all the hydrogen ions in the solution have been used up, and no other positive ions are left which can take over their job. The corrosive effects of stray current can be easily demonstrated as follows, after passing a DC current through the cell containing a 8% concentration NaCl solution, the formation of hydrogen bubbles is readily visible on the rebars connected to the negative post of the DC power supply while the rebars connected to the positive post shows signs of rapid corrosion.

4. TEST RESULTS AND DISCUSSIONS

4.1. Durability of RA-SC Concrete under Sulfates Attack

The hardened concrete properties of the RA-SC concrete mixes are studied under the effect of sulfates at different ages 2, 4 and 6 months. The samples are immersed in a sodium sulfate solution *(with 8% concentration degree).*

The results of the compressive, the tensile splitting and the flexure strength tests due to the attack of sulfates are shown in Table (8) and Figures (7) to (9).

Table 8. Hardened concrete properties of "RA-SC" concrete under the effect of sulfates.

Mix code	Compressive Strength *(MPa)*	Tensile Strength *(MPa)*	Flexural Strength *(MPa)*
DS-0	44	3.503	5.287
DS-2	47	3.598	5.7
DS-4	52.5	3.726	6
DS-6	43	3.312	5.22
CS-0	35	2.738	4.125
CS-2	36	2.866	4.575
CS-4	39	3.184	5.1
CS-6	32.7	2.707	3.9
BS-0	27.5	2.707	3.825
BS-2	29	2.802	4.2
BS-4	30.5	3.025	4.425
BS-6	24	2.388	3.45

Figure (7) shows the effect of sulfate attack on the compressive strength values for the tested samples after different exposure periods of sulfate attack. The values of the compressive strength increase under the effect of sulfates at early ages. That may because the attack products deposited in the pore spaces of concrete. After 4 months values started to decrease and the damage rate of concrete has been greatly accelerated. In the case of the self-curing concrete cast using dolomite, the compressive strength increases by about 6.8% and 19.3% at 2 and 4 months, respectively, then decreases by 2.3% at 6 months compared to the control mix "DS-0" which not attacked. In the case of the self-curing concrete made from crushed concrete, the compressive strength increases by about 2.9% and 11.4% at 2 and 4 months, respectively, then decrease by 6.6% at 6 months compared to the control mix "CS-0". The lower value of obtained compressive strength of samples cast using crushed concrete compared to those cast using dolomite is thought to be due to an excessive amount of voids and the lower crushing factor of crushed concrete. In the case of self-curing concrete cast using crushed red bricks, the compressive strength increases by about 5.5% and 10.9% at 2 and 4 months, respectively, then decrease by 12.7% at 6 months compared to the control mix "BS-0". The loss of compressive strength of crushed red bricks compared to dolomite is thought to be due to the higher number of voids and higher permeability of red bricks which lead to a greater area of material being attacked by the sulfates. The results in good agreement with previous researchers [16].

Table 9. Bond strength values of "RA-SC" concrete under the effect of chlorides.

Mix Code	Bond Strength *(MPa)*		
	Control (28 days)	1 month	2 months
DC	14.994	13.933	12.208
CC	12.606	11.677	9.952
BC	10.615	9.952	7.961

Table 10. Initial cracking loads and ultimate loads for tested beams.

Beam Samples	Load *(kN)*	
	Initial Cracking Load (P_{cr})	Ultimate Load (P_u)
DC-0	20.0	67.25
CC-0	14.0	67.9
BC-0	10.0	57.35
DC-1	13.0	59.95
CC-1	11.0	62.1
BC-1	8.0	53.1
DC-2	10.0	56.75
CC-2	9.0	51.8
BC-2	6.0	44.9

Figure (8) shows the tensile splitting strength values after different exposing times under the effect of sulfate attack. It is found that the results in good agreement with those of compressive strength. In the case of using dolomite at self-curing concrete, the tensile splitting strength increases by about 2.7% and 6.4% at 2 and 4 months, respectively, then decreases by about 5.5% at 6 months compared to the control mix "DS-0". In the case of the self-curing concrete made from crushed concrete, the tensile splitting strength increases by about 4.7% and 16.3% at 2 and 4 months, respectively, then decreases by about 1.1% at 6 months compared to the control mix "CS-0". In the case of self-curing concrete cast using crushed red bricks as recycled coarse aggregate the tensile splitting strength increases by about 3.5% and 11.7% at 2 and 4 months, respectively, then decreases by about 11.8% at 6 months compared to the control mix "BS-0".

Figure (9) shows the flexure strength values at different times under the effect of sulfates. The flexure strength values increase under the effect of sulfates at 2 and 4 months, then start to decrease at 6 months *(in the range of this study)*. In the case of self-curing concrete cast using dolomite as coarse aggregate, the flexure strength increases by about 7.8% and 13.5% at 2 and 4 months, respectively, then decreases by about 1.3% at 6 months compared to the control mix "DS-0". In the case of the self-curing concrete made from crushed concrete, the flexure strength increases by about 10.9% and 23.6% at 2 and 4 months, respectively, then decreases by about 5.5% at 6 months compared to the control mix "CS-0". In the case of self-curing concrete cast using crushed red bricks as recycled coarse aggregate, the flexure strength increases by about 9.8% and 15.7% at 2 and 4 months, respectively, then decrease by 9.8% at 6 months compared to the control mix "BS-0". The results are satisfying previous researches [16].

4.2. Durability of RA-SC Concrete under Chlorides Attack

The bond strength of the RA-SC concrete mixes and the flexure behavior of the "RA-SC" reinforced concrete beams are studied under the effect of chloride attack for different exposure periods (1 and 2 months). Chloride effect is accelerated by using an electrical cell and by using a high dosage of chlorides (8% concentration degree as about 20% of allowable dosage at E.C.P. 203/2007 [19]).

4.2.1. Effects of Chlorides on Bond Strength

Table (9) and Fig. (10) show the bond strength values at different periods under the effect of chloride attacks. Based on Fig. (10), the bond strength values decrease over the time under the effect of chlorides. In the case of self-curing concrete cast using dolomite as coarse aggregate, the bond strength decreases by about 7.1% and 18.6% at 1 and 2 months, respectively. That may because the penetrations of chloride ions to the protective oxide film then leave the steel vulnerable to corrosion. Due to the formation of corrosion the bond between the concrete and reinforcement lost. In the case of the self-curing concrete made from crushed concrete, the bond strength decreases by about 7.4% and 21% at 1 and 2 months, respectively. In the case of self-curing concrete cast using crushed red bricks as recycled coarse aggregate, the bond strength decreases by about 6.2% and 25% at 1 and 2 months, respectively.

4.2.2. Effects of Chlorides on Flexure Behavior of RA-SC Reinforced Concrete Beams

Beams are tested using four-point load flexure test as shown in Figs. (5) and (6). Beam failures can be caused by different factors and reasons, and the most common causes of beam failures are shear stress and bending stress.

4.2.2.1. Initial cracking and ultimate loads

Initial cracking and ultimate loads of all tested beams are listed in Table (10) and shown in Fig. (11). The initial cracking and ultimate loads of the "RA-SC" reinforced concrete beams decrease over the time under the effect of chlorides attack.

The initial cracking and ultimate loads of the self-curing concrete beams with dolomite aggregates "DC" are higher than both self-curing concrete beams cast using crushed concrete "CC" or cast using crushed red bricks "BC". That may refer to the loss of bond between the rebars and the concrete due to the corrosion. Those values are satisfied Bashandy et al., 2016 [23].

4.2.2.2. Load-Deflection Curves

A- Deflection at mid-span of beam "point A".

The results of self-curing reinforced concrete beams cast using dolomite "DC", crushed concrete "CC", and crushed bricks "BC" are shown in Fig. (12).

The obtained results for the control group (tested after 28 days without chlorides effect) are shown in Figs. (13) to (15). Based on test results, the ductility of the reinforced self-curing beams cast using dolomite "DC-0" is lower than both reinforce self-curing beams cast using crushed concrete "CC-0" and crushed bricks "BC-0" beams by about 30.2% and 70.9%, respectively. After immersing in accelerated chloride attack for one month, the ductility of the reinforced self-curing beams cast using dolomite "DC-1" is lower than both the reinforced self-curing beams cast using crushed concrete "CC-1" the reinforced self-curing beams cast using crushed red bricks "BC-1" by about 10.2% and 31.1%, respectively. After 2 months, the ductility of the reinforced self-curing beams cast using dolomite "DC-2" is lower than both the reinforced self-curing beams cast using crushed concrete "CC-2" the reinforced self-curing beams cast using crushed red bricks "BC-2" by about 0.5% and 7.1%, respectively. That may because the weakness of crushed red bricks as coarse aggregate compared to dolomite.

It is observed that the stiffness increases when the ductility ratio decreases. For control beams which tested after 28 days, the stiffness of the reinforced self-curing beams cast using dolomite "DC-0" is higher than both reinforce self-curing beams cast using crushed concrete "CC-0" and crushed bricks "BC-0" beams by about 1% and 16.6%, respectively. After one month under accelerated chloride attack, the stiffness of the reinforced self-curing beams cast using dolomite "DC-1" is higher than both the reinforced self-curing beams cast using crushed concrete "CC-1" the reinforced self-curing beams cast using crushed red bricks “BC-1” by about 1% and 17.5%, respectively. After 2 months, the stiffness of the reinforced self-curing beams cast using dolomite "DC-2" is higher than both the reinforced self-curing beams cast using crushed concrete "CC-2" the reinforced self-curing beams cast using crushed red bricks "BC-2" by about 10.8% and 18.7%, respectively.

Based on Figs. (16) to (18), the ductility values increase over the time under the effect of chlorides. For "DC" beam group which cast using dolomite, the ductility increases by about 47.3% and 87%, respectively, after exposing to chlorides for 1 and 2 months compared to control beams. For crushed concrete "CC" beams, the ductility increases by about 24.6% and 44.3%, respectively, after exposing to chlorides for 1 and 2 months compared to control beams. For crushed bricks "BC" beams, the ductility increases by about 13% and 17.2%, respectively, after exposing to chlorides for 1 and 2 months.

The stiffness values decrease over the time under the effect of chlorides. The stiffness decrease when the ductility ratio increases. The decrease is faster for quicker loading rate. For dolomite beams "DC" the stiffness decreases by about 10.6% and 14.4% at 1 and 2 months respectively. For crushed concrete beams "CC" the stiffness decreases by about 10.6% and 23% at 1 and 2 months respectively. For crushed bricks beams "BC" the stiffness decreases by about 11.6% and 16.6% at 1 and 2 months respectively.

B- Deflection at span quarter of beam "point B".

The results of load-deflection curves at the quarter span of beams at different load stages for dolomite beams "DC", crushed concrete beams "CC" and crushed bricks beams "BC" are shown in Fig. (19).

Based on Figs. (20) to (22) for the control group, the deflection at the initial cracking load for dolomite beams "DC-0" is lower than both reinforce self-curing beams cast using crushed concrete "CC-0" and crushed bricks "BC-0" beams by about 12.8% and 34.8%, respectively. After exposing for 1 month, the deflection at the initial cracking load for the reinforced self-curing beams cast using dolomite "DC-1" is lower than both the reinforced self-curing beams cast using crushed concrete "CC-1" the reinforced self-curing beams cast using crushed red bricks "BC-1" by about 13.9% and 43%, respectively. After exposing for 2 months, the deflection at the initial cracking load for the reinforced self-curing beams cast using dolomite "DC-2" is lower than both the reinforced self-curing beams cast using crushed concrete "CC-2" the reinforced self-curing beams cast using crushed red bricks "BC-2" by about 12.5% and 27.5%.

Based on Figs. (23) to (25), the deflection at the initial cracking load of control (tested after 28 days without exposing to chlorides effect) dolomite beams "DC-0" increases by about 21.9% and 61.3% respectively, after 1 and 2 months. The deflection values at the initial cracking load for reinforced self-curing beams cast using crushed concrete "CC-0" increases by about 8.1% and 10.2%, respectively, after 1 and 2 months. The deflection values at the initial cracking load of reinforced self-curing beams cast using crushed red brick "BC-0" increases by about 51.7% and 75.8%, respectively at 1 and 2 months.

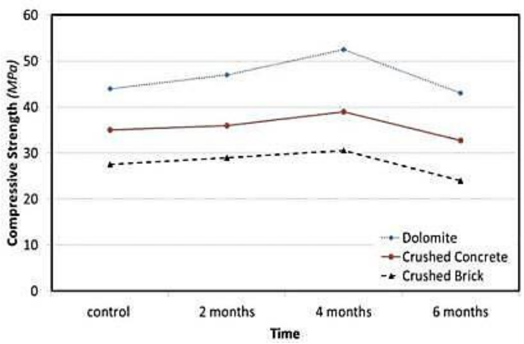

Fig. 7. The compressive strength values at different times under the attack of sulfates.

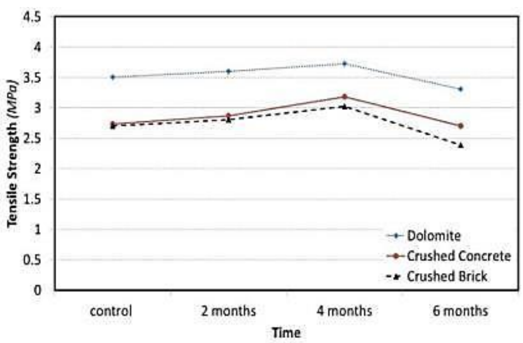

Fig. 8. The splitting tensile strength values at different times under the attack of sulfates.

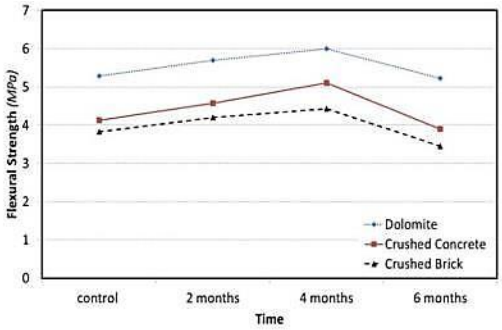

Fig. 9. The flexure strength values at different times under the attack of sulfates.

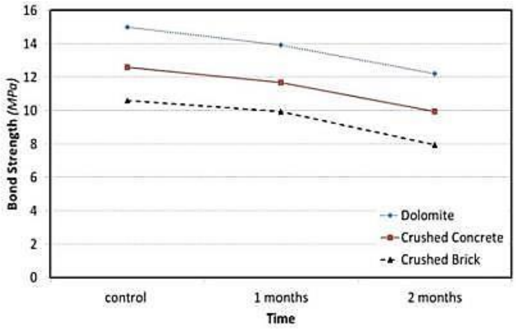

Fig. 10. The bond strength values at different times under the attack of chlorides.

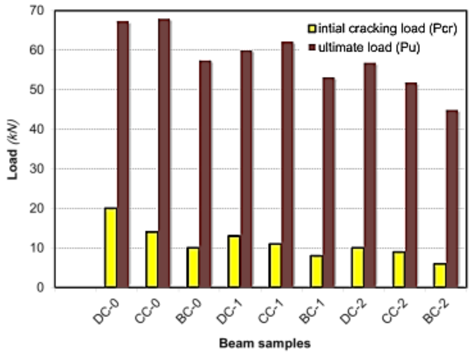

Fig. 11. The initial cracking and the ultimate loads for tested beams.

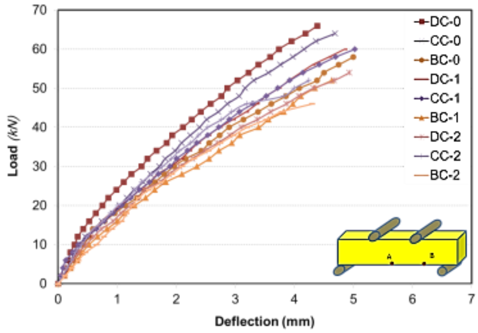

Fig. 12. Load-deflection curves at the mid span of "RA-SC" reinforced concrete beams at different ages.

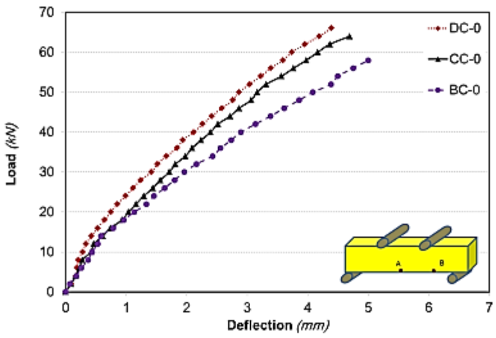

Fig. 13. Load-deflection curves at mid span for control "RA-SC" reinforced concrete beams (after 28 days).

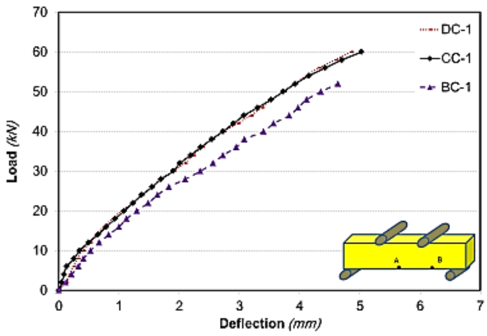

Fig. 14. Load-deflection curves at the mid span of "RA-SC" reinforced concrete beams immersed at accelerated chloride effect for 1 month.

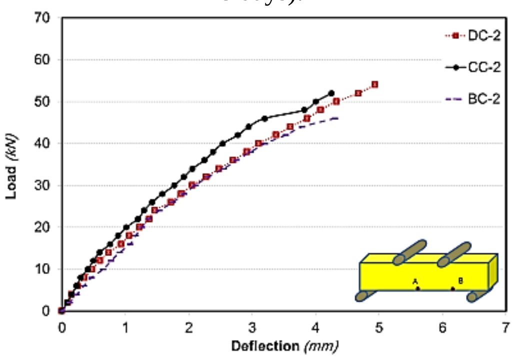

Fig. 15. Load-deflection curves at the mid span of "RA-SC" reinforced concrete beams immersed at accelerated chloride effect for 2 months.

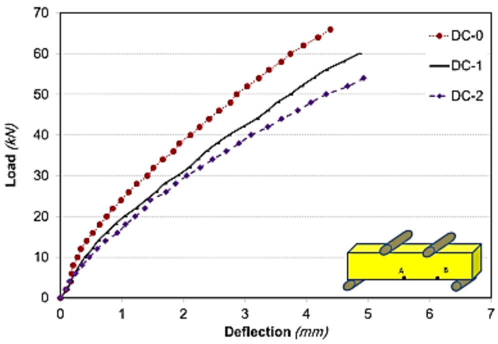

Fig. 16. Load-deflection curves at the mid span of reinforced self-curing concrete beams cast using dolomite at different ages.

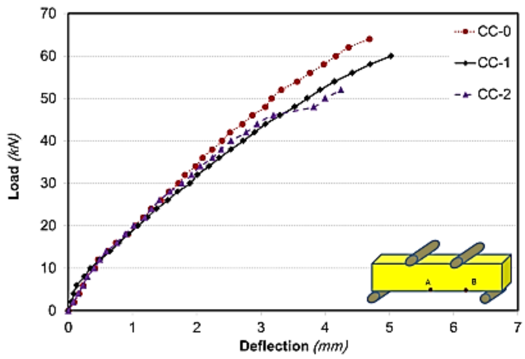

Fig. 17. Load-deflection curves at the mid span of reinforced self-curing concrete beams cast using crushed concrete at different ages.

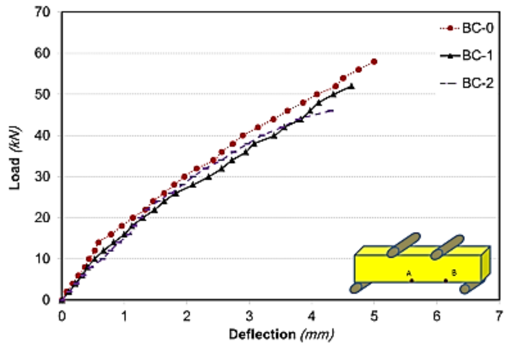

Fig. 18. Load-deflection curves at the mid span of reinforced self-curing concrete beams cast using crushed bricks at different ages.

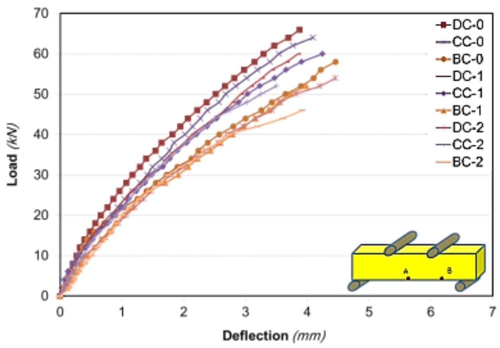

Fig. 19. Load-deflection curves at a span quarter of "RA-SC" reinforced concrete beams for different exposing periods.

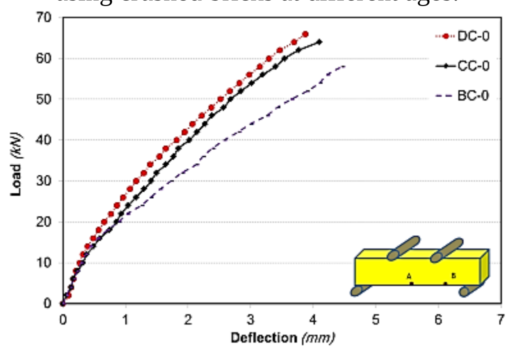

Fig. 20. Load-deflection curves for control beam samples at a span quarter of "RA-SC" reinforced concrete beams (at 28 days).

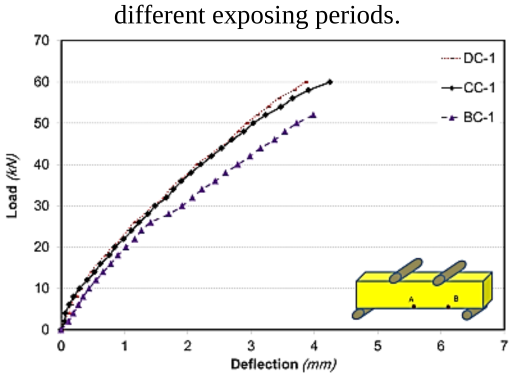

Fig. 21. Load-deflection curves at a span quarter of "RA-SC" reinforced concrete beams after 1 month of accelerated effects of chlorides.

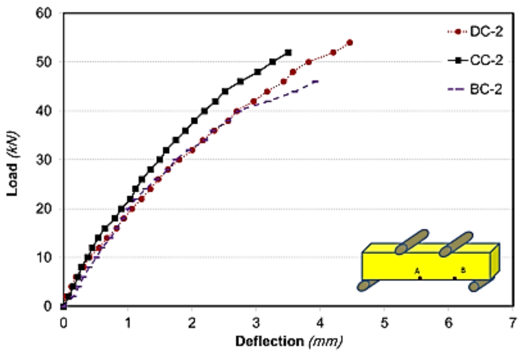

Fig. 22. Load-deflection curves at a span quarter of "RA-SC" reinforced concrete beams after 2 months of accelerated effects of chlorides.

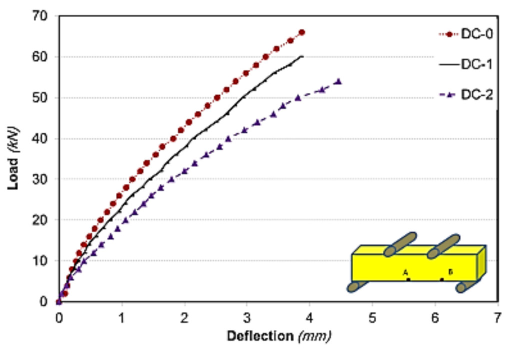

Fig. 23. Load-deflection curves at a span quarter of reinforced self-curing concrete beams cast using dolomite after different exposure periods.

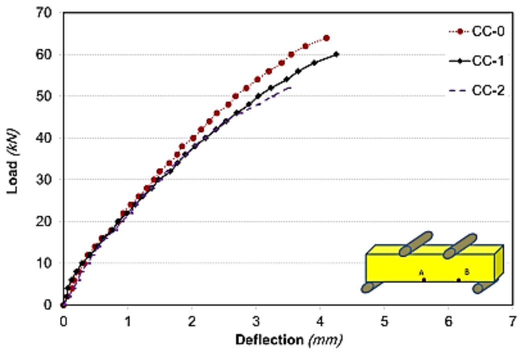

Fig. 24. Load-deflection curves at a quarter of the span of reinforced self-curing concrete beams cast using crushed concrete after different exposure periods.

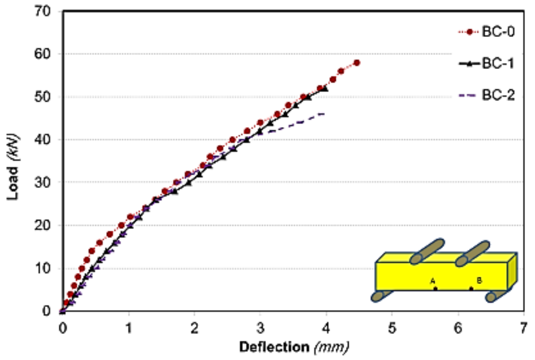

Fig. 25. Load-deflection curves at a quarter of the span of reinforced self-curing concrete beams cast using crushed bricks after different exposure periods.

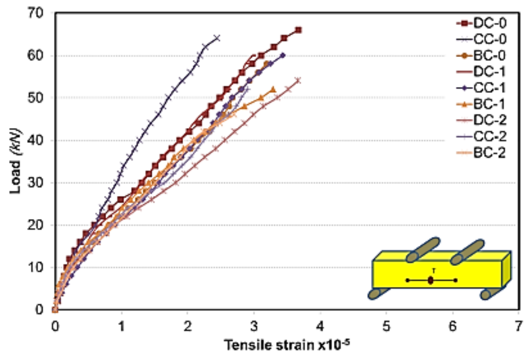

Fig. 26. Load-tensile strain curves of "RA-SC" reinforced concrete beams at different ages.

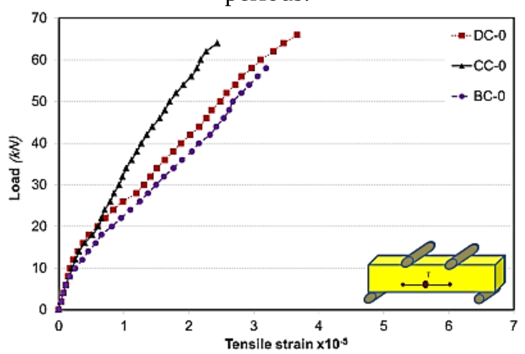

Fig. 27. Load-tensile strain curves of "RA-SC" reinforced concrete beams for control samples.

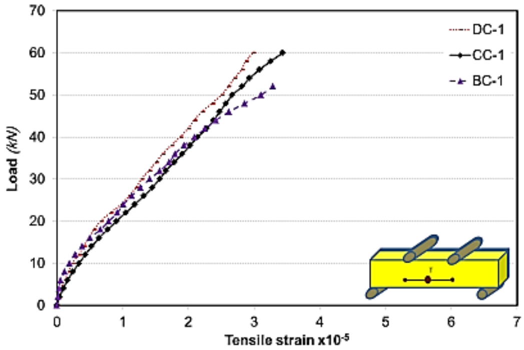

Fig. 28. Load-tensile strain curves of "RA-SC" reinforced concrete beams after 1 month of accelerated effects of chlorides.

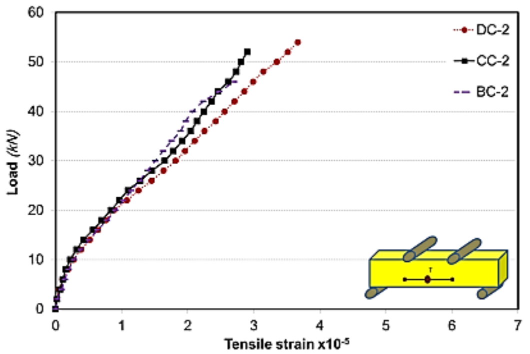

Fig. 29. Load-tensile strain curves of "RA-SC" reinforced concrete beams after 2 months of accelerated effects of chlorides.

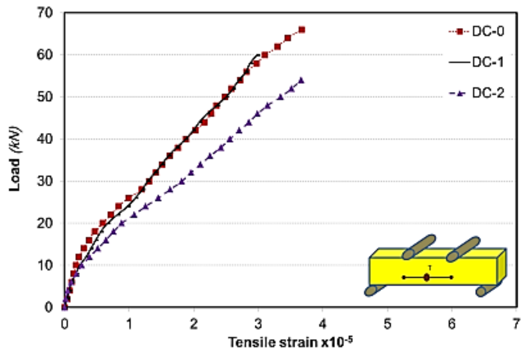

Fig. 30. Load-tensile strain curves of reinforced self-curing concrete beams cast using dolomite after different exposure periods.

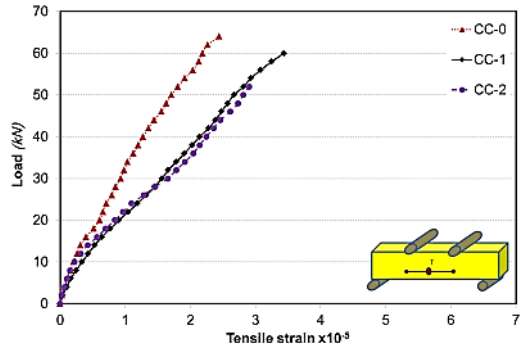

Fig. 31. Load-tensile strain curves of reinforced self-curing concrete beams cast using crushed concrete after different exposure periods.

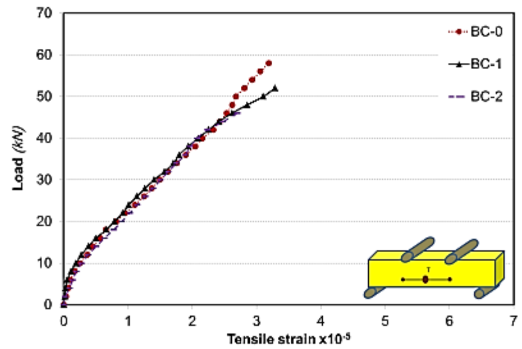

Fig. 32. Load-tensile strain curves of reinforced self-curing concrete beams cast using crushed red bricks after different exposure periods.

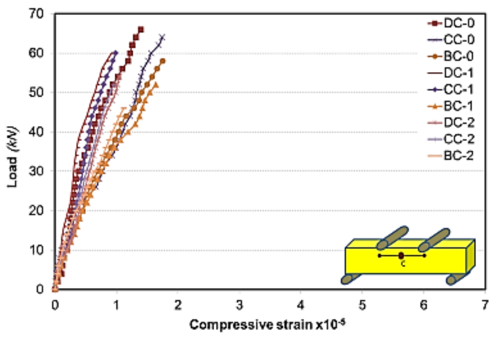

Fig. 33. Load-compressive strain curves of "RA-SC" reinforced concrete beams after different exposure periods.

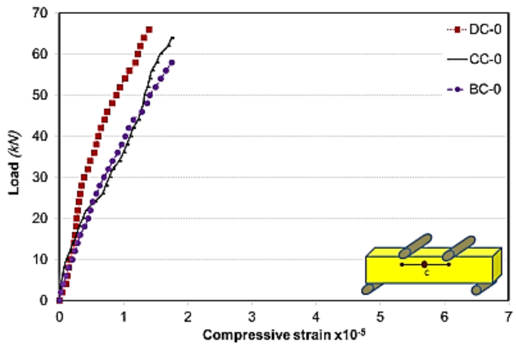

Fig. 34. Load-compressive strain curves of "RA-SC" reinforced concrete beams for control samples.

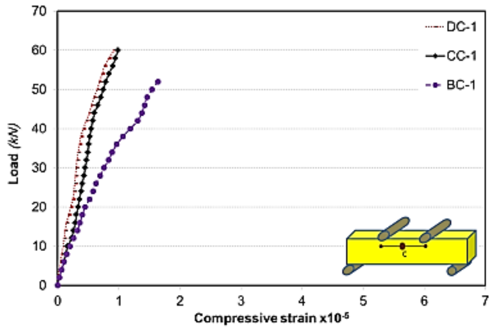

Fig. 35. Load-compressive strain curves of "RA-SC" reinforced concrete beams after 1 month.

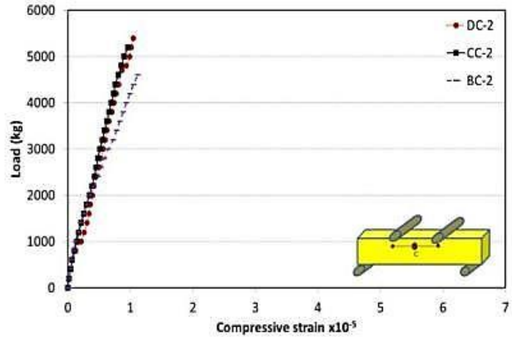

Fig. 36. Load-compressive strain curves of "RA-SC" reinforced concrete beams after 2 months.

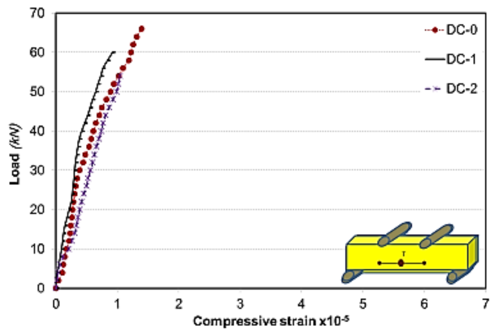

Fig. 37. Load-compressive strain curves of reinforced self-curing concrete beams cast using crushed dolomite after different exposure periods.

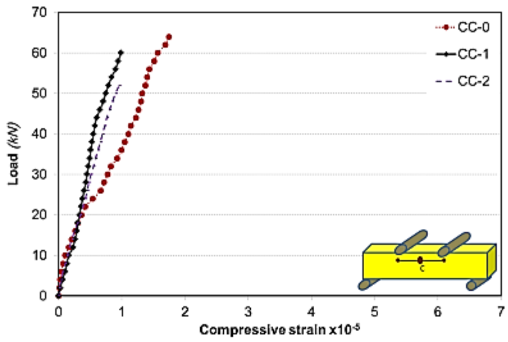

Fig. 38. Load-compressive strain curves of reinforced self-curing concrete beams cast using crushed concrete after different exposure periods.

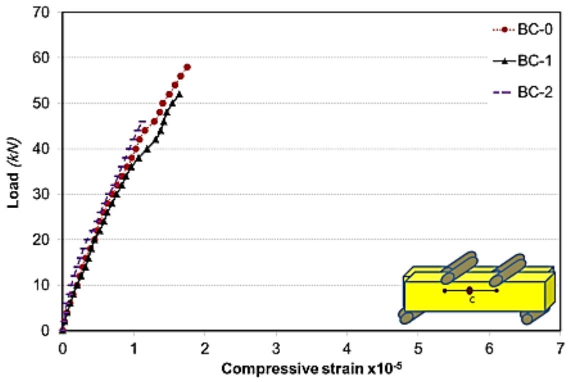

Fig. 39. Load-compressive strain curves of reinforced self-curing concrete beams cast using crushed bricks after different exposure periods.

4.2.2.3. Load-Strain curves

A- Strain at bottom "tensile strain".

The results of load-strain curves at bottom "tensile strain" of beams after different periods for dolomite beams "DC", crushed concrete beams "CC" and crushed bricks beams "BC" are shown in Fig. (26).

Based on Figs. (27) to (29), for the control group (tested after 28 days without chlorides effect) the elastic modulus of the reinforced self-curing beams cast using dolomite "DC-0" is higher than both reinforce self-curing beams cast using crushed concrete “CC-0” and crushed bricks "BC-0" beams by about 25.9% and 38.1% respectively. After immersing in accelerated chloride effect for one month, the elastic modulus of the reinforced self-curing beams cast using dolomite "DC-1" is higher than both the reinforced self-curing beams cast using crushed concrete “CC-1” the reinforced self-curing beams cast using crushed red bricks “BC-1” by about 3.6% and 15.1%, respectively. After 2 months, the elastic modulus of the reinforced self-curing beams cast using dolomite "DC-2" is higher than both the reinforced self-curing beams cast using crushed concrete “CC-2” the reinforced self-curing beams cast using crushed red bricks “BC-2” by about 8.6% and 14.6%, respectively.

Also, the modulus of toughness of dolomite beams is higher than both the crushed concrete beams and crushed bricks beams. For control beams which tested after 28 days, the modulus of toughness of dolomite beams "DC-0" is higher than both reinforce self-curing beams cast using crushed concrete “CC-0” and crushed bricks "BC-0" beams by about 11.9% and 26%, respectively. After one month under accelerated chloride attack, the modulus of toughness of dolomite beams "DC-1" is higher than both the reinforced self-curing beams cast using crushed concrete “CC-1” the reinforced self-curing beams cast using crushed red bricks “BC-1” by about 19.6% and 23%, respectively. After 2 months, the modulus of toughness of dolomite beams "DC-2" is higher than both the reinforced self-curing beams cast using crushed concrete “CC-2” the reinforced self-curing beams cast using crushed red bricks “BC-2” by about 15.1% and 34.9%, respectively.

Based on Figs. (30) to (32), the elastic modulus values decrease over the time under the effect of chlorides. For dolomite "DC" beams group, the elastic modulus decreases by about 33.2% and 41.4%, respectively, after exposing to chlorides for 1 and 2 months compared to control beams. For crushed concrete "CC" beams, the elastic modulus decreases by about 13% and 27.7%, respectively, after exposing to chlorides for 1 and 2 months compared to control beams. For crushed bricks "BC" beams, the elastic modulus decreases by about 8.3% and 19.1%, respectively, after exposing to chlorides for 1 and 2 months.

Also, the modulus of toughness decreases over the time under the effect of chlorides. For dolomite beams "DC" the modulus of toughness decreases by about 11.1% and 26.9% at 1 and 2 months respectively. For crushed concrete beams "CC" the modulus of toughness decreases by about 18.9% and 29.6% at 1 and 2 months respectively. For crushed red brick beams "BC", the modulus of toughness decreases by about 7.6% and 35.7% at 1 and 2 months respectively.

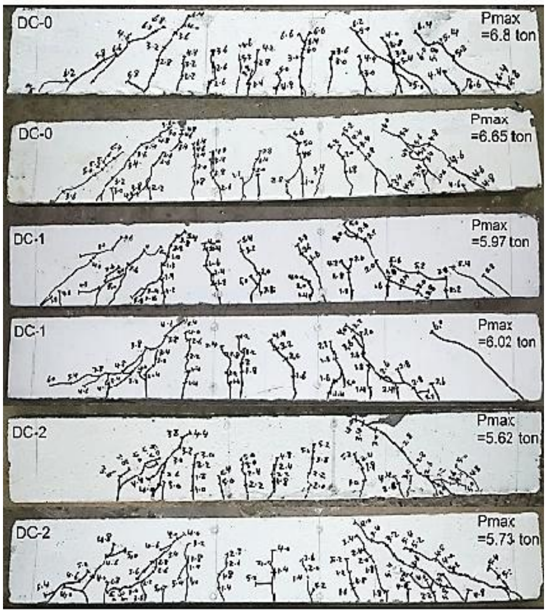

Fig. 40. Crack patterns for self-curing beams cast using dolomite after chloride attack.

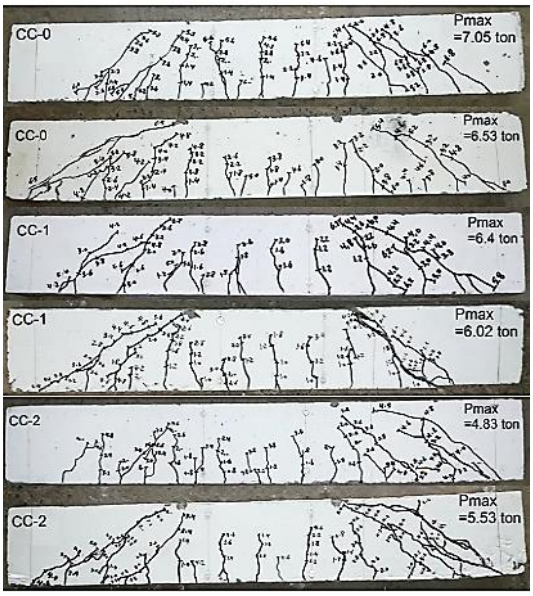

Fig. 41. Crack patterns for self-curing beams cast using crushed concrete after chloride attack.

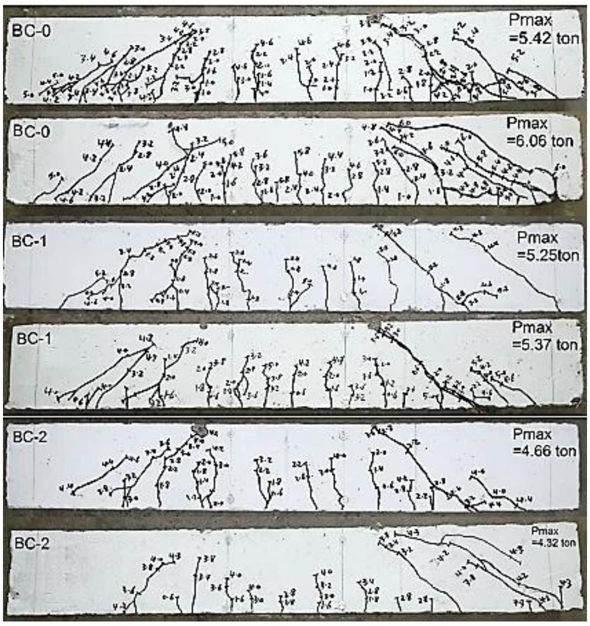

Fig. 42. Crack patterns for self-curing beams cast using crushed bricks after chloride attack.

B- Strain at top "compressive strain".

The results of load-strain curves at the upper layer "compressive strain" of beams at different ages for dolomite beams "DC", crushed concrete beams "CC" and crushed bricks beams "BC" are shown in Fig. (33).

The results of load-strain curves at the upper layer (far about 1.5 cm of the top) which refer as the compressive strain for control beams, beams immersed for 1 and 2 months are shown in Figs. (34) to (36). The results of load-strain curves at top "compressive strain" of beams at different ages under the chlorides effect for dolomite beams "DC", crushed concrete beams "CC" and crushed bricks beams "BC" are shown in Figs. (37) to (39).

4.2.2.4. Crack pattern

The crack patterns are recorded and illustrated at each load increment up to failure then photographed. The number of cracks increased during loading stages. Figures from (40) to (42) show the crack patterns for dolomite "DC", crushed concrete "CC" and crushed bricks "BC" self-curing concrete beams at different loading stages for different periods at 28day as control samples, 1, and 2 months.

5. CONCLUSIONS

Based on the experimental results presented in this study, the following conclusions could be drawn as follows:

1. The durability of the self-curing concrete cast using dolomite aggregate is higher than both self-curing concretes with crushed concrete and crushed bricks as aggregates.

2. The compressive, tensile splitting and flexure strength values increase under the effect of sulfates at 2 and 4 months, then starts to decrease at 6 months *(in the range of this study)*.

3. The bond strength values of reinforced RA-SC concrete decrease over the time under the effect of chlorides.

4. The initial cracking and ultimate loads of the "RA-SC" reinforced concrete beams decrease over the time under the effect of chlorides attack.

5. The initial cracking and ultimate loads of the self-curing concrete beams with dolomite aggregate "DC" are higher than both self-curing concrete beams with crushed concrete aggregate "CC" and self-curing concrete beams with crushed red bricks aggregate "BC".

6. The flexure strength of the "RA-SC" reinforced concrete beams decrease over the time under the attack of chlorides due to the forming of corrosion at steel reinforcing bars.

7. The ductility values of the "RA-SC" reinforced concrete beams increase over the time under the effect of chlorides. The ductility of DC beams is lower than both CC and BC beams.

8. It is observed that the stiffness decrease when the ductility ratio increases. The rate of decrease is faster when the loading rate is faster. The stiffness of DC beams is higher than both the CC beams and BC beams.

9. The elastic modulus values of the "RA-SC" reinforced concrete beams decreases over the time under the attack of chlorides. The elastic modulus of DC beams is higher than both CC beams and BC beams.

10. The modulus of toughness decreases over the time under the effect of chlorides. The modulus of toughness of DC beams is higher than both CC and BC beams.

Finally, it can be concluded that recycled aggregates such as (crushed concrete and crushed red bricks) can be used in self-curing concrete with satisfied durability characteristics under chlorides and sulfate attacks. Dolomite then crushed concrete followed by crushed red bricks can be used are suggested as coarse aggregate for self-curing concrete. Also, using recycled aggregates decrease environmental impact and save natural resources. Chemical curing agents (such as PEG 400) are used to reduce the water evaporation from the concrete, and hence increase the water retention capacity of concrete compared to conventional concrete.

REFERENCES

1 Padmini AK, Ramamurthy K, Mathews MS, Influence of Parent Concrete on the Properties of Recycled Aggregate Concrete, *Construction and Building Materials,* Vol. 23(2), 2009, pp. 829-836.

2 Gomez-Soberon JMV, Porosity of Recycled Concrete with Substitution of Recycled Concrete Aggregate, *Cement and Concrete research*, Vol. 32, 2002, pp. 1301-1311.

3 Ryu JS, Improvement on Strength and Impermeability of Recycled Concrete Made from Crushed Concrete Coarse Aggregate, *Journal of Materials Science Letters*, Vol. 21, 2002, pp. 1565-1567.

4 Spoon CS, Shi ZH, Lam L, Effect of Microstructure of ITZ on Compressive Strength of Concrete Prepared with Recycled Aggregate, *Construction and Building Materials*, Vol. 18, No. 6, 2004, pp. 461-468.

5 EL-Dieb AS, Okba SH, Performance of Self Curing Concrete, M. Sc. Thesis, Ain Shams University, Cairo, Egypt, 2005.

6 Bentz DP, Lura P, Roberts JW, Mixture Proportioning for Internal Curing, *Concrete International*, Vol. 27, Vol. 2, 2005, pp. 35-40.

7 Bilek V, Kersner Z, Schmid P, Mosler T, The Possibility of Self-Curing Concrete, In: International Conf. of Innovations and Developments in Concrete Materials and Construction, 2002, UK.

8 Dhir RK, Hewlett PC, Dyer TD, Mechanisms of Water Retention in Cement Pastes Containing a Self-Curing Agent, *Magazine of Concrete Research*, Vol. 50, Vol. 1, 1998, pp. 85-90.

9 Kovler K, Bentur A, Zhutovsky S, Efficiency of Lightweight Aggregates for Internal Curing of High Strength Concrete to Eliminate Autogenous Shrinkage, *Material and Structure*, Vol. 34, Vol. 246, 2002, pp. 97-101.

10 Hammer TA, Bjontegaard O, Sellevold EJ, Internal Curing Role of Absorbed Water in Aggregates: High-performance Structural Lightweight Concrete, *ACI Fall Convention* ACI SP 218, 2002.

11 Geiker MR, Bentz DP, Jensen OM, Mitigating Autogenous Shrinkage by Internal Curing," High Performance Structural Lightweight Concrete, *American Concrete Institute*, 2004, pp. 143-150.

12 Lura P, Autogenous Deformation and Internal Curing of Concrete, Delft, The Netherlands: Ph. D. Thesis, Technical University Delft, 2003.

13 Collepardi M, Borsoi A, Collepardi S, Ogoumah, Olagot JJ, Troli R, Effects of Shrinkage Reducing Admixture in Shrinkage Compensating Concrete Under Non-Wet Curing Conditions, Cement Concrete Composites, 2005.

14 Kosmatka SH, Kerkhoff B, Panarese WC, Design and control of concrete mixtures, Portland Cement Association of Canada, 7th Ed., 2002, pp. 100-104.

15 Ann KY, Durability of Recycled Aggregate Concrete Using Pozzolanic Materials, *Waste Management*, 2008.

16 Bashandy AA, Self-curing Concrete under Sulfate Attack, Archives of Civil Engineering, Vol. 62, Vol. 2, 2016,

17 Kim H, Bentz D, Internal Curing with Crushed Returned Concrete Aggregates for High Performance Concrete, NRMCA Concrete Technology Forum, 2008, pp. 1-12.

18 E.S.S.4756-1/2009, Portland Cement, Ordinary and Rapid Hardening, Egyptian Standard Specification, Ministry of Industry, Cairo, Egypt, 2009.

19 E.C.P.203/2007, Egyptian Code of Practice: Design and Construction for Reinforced Concrete Structures, Housing and Building National Research Centre, Cairo, Egypt, 2007.

20 ASTM.C-33, Aggregates, Philadelphia, USA: American Society for Testing and Materials ASTM International, 2003.

21 E.S.S.262/2011. Egyptian Standard Specification for Steel Bars, Ministry of Industry, Cairo, Egypt, 2011.

22 ASTM.C-494, Chemical Admixtures for Concrete, American Society for Testing and Materials ASTM International, Philadelphia, USA, 2015.

23 Bashandy AA, Safan MA, Ellyien MM, Feasibility of Using Recycled-Aggregates in Self-Curing

Concrete, In: The 9th Alexandria International Conference on Structural and Geotechnical Engineering, 2016, Alexandria, Egypt.

24 Ellyien MM, Durability of Recycled Aggregate Self-curing Concrete, M. Sc. Thesis, F. of Engineering, Menofia University, Menoufia, Egypt, 2015.

25 Bashandy AA, The Feasibility of Protect Rebars Against Corrosion Using Locally Available Materials in Egypt, In: The 9th International Conference on Civil and Architecture Engineering ICCAE-9, 2012, Cairo, pp. 29-31.

26 Kauffman AM, Understanding Electrochemical Cells, Solartron, 1997, *(Available from: http://www.solartron.com)*.

27 González JA, Miranda JM, Birbilis N, Feliu S, Electrochemical Techniques for Studying Corrosion of Reinforcing Steel: Limitations and Advantages, *Corrosion*, 2005, Vol. 61, No. 1, pp. 37-50.

28 Emam EA, Durability of Self-Curing Concrete, M. Sc. at Faculty of Engineering, Menoufia University, Menoufia, Egypt, 2012.

29 E.S.S.1109/2008, Aggregate, Ministry of Industry, Cairo, Egypt, 2008.